Underwater Soft Robotics, the Benefit of Body-Shape Variations in Aquatic Propulsion

Francesco Giorgio-Serchi and Gabriel D. Weymouth

Abstract Aquatic organisms capable of undergoing extensive volume variation of their body during locomotion can benefit from increased thrust production. This is enabled by making use of not only the expulsion of mass from their body, as documented extensively in the study of pulsed-jet propulsion, but also from the recovery of kinetic energy via the variation of added mass. We use a simplified mechanical system, i.e. a shape-changing linear oscillator, to investigate the phenomenon of added-mass recovery. Our study proves that a deformable oscillator can be set in sustained resonance by exploiting the contribution from shape variation alone which, if appropriately modulated, can annihilate viscous drag. By confirming that a body immersed in a dense fluid which undergoes an abrupt change of its shape experiences a positive feedback on thrust, we prove that soft-bodied vehicles can be designed and actuated in such a way as to exploit their own body deformation to benefit of augmented propulsive forces.

1 Introduction

Most aquatic organisms rely on periodic oscillations of some wing-link control surface for locomotion. These may entail fins, a tail or whole-body ondulatory routines, which eventually participate in generating rotating fluids which is pushed backwards while propelling the body forwards [8, 14]. A broad degree of variability is found in the details of the kinematics of the surfaces of actuation and the associated topology of the vortices generated; however, the processes which enable vertebrate organisms to propel themselves in water manifest a remarkable degree of consistency [13].

Of higher interest within the frame of soft robotics are those mode of locomotion where body modifications don't necessarily rely on the activation of joints or the

Giorgio-Serchi (✉) · G.D. Weymouth
Fluid Structure Interaction, Southampton Marine and Maritime Institute,
University of Southampton, Boldrewood Campus, Southampton SO16 7QF, UK
e-mail: f.giorgio-serchi@soton.ac.uk

G.D. Weymouth
e-mail: g.d.weymouth@soton.ac.uk

C. Laschi et al. (eds.), *Soft Robotics: Trends, Applications and Challenges*,
Biosystems & Biorobotics 17, DOI 10.1007/978-3-319-46460-2_6

coordinated motion of reciprocating limbs, but rather those where the body undergoes extensive transformation of its topology or volume. In this respect, mono-cellular organisms or aggregate of these, as well as certain tunicate and cephalopods [6], are better paradigms of what a soft body, and hence a soft robot, can achieve [15]. These organisms have attracted the attention of the robotics community because they represent the perfect source of inspiration for the design of soft-bodied underwater vehicles [3, 12]. In the past, cephalopods have been studied extensively for their pulsed-jet propulsion [7], but lately their volume-changing propulsion routine has been associated with the phenomenon of added-mass recovery and the idea that this may further contribute to the thrust production [16, 17]. If confirmed, this would have a major impact both on the understanding of the biomechanics of these living organisms, as well as on the chance to exploit this principles in the design and control of innovative underwater vehicles [2, 4, 11]. Following the results of [5], we report on the phenomenon of added-mass recovery for a simplified mechanical system in order to demonstrate that shape variation can indeed act as a secondary source of thrust.

2 Added Mass Variation as a Thrust Term

When a body is accelerating in a dense medium, added mass defines an inertial term which depends on the amount of kinetic energy lost for accelerating the fluid around it. This was first postulated by Alfred Barnard Basset [1] in attempting to account for the differing frequencies experienced by a body oscillating in vacuum and in a dense fluid. Given the dynamics of a 1 dof (degrees of freedom) oscillator,

$$m^*\ddot{x} + kx = 0, \tag{1}$$

where m^*, $x(t)$ and k respectively represent the effective mass, the position and the elastic constant of the oscillator, the frequencies of oscillation in vacuum, ω_0, and in a dense medium, ω^*, are defined as $\omega_0 = \omega^* = \sqrt{k/m^*}$. However, while for the case of a body oscillating in vacuum $m^* \equiv m$, for a body vibrating in a dense fluid $m^* = m + m_a$, where m_a is the added mass of the body, thus explaining why $\omega^* \leq \omega_0$.

The added-mass is thus a force generated by the fluid acting against the acceleration of a body and, for single bodies far away from solid boundaries, it depends on the density of the fluid and the shape of the body. This term is especially important in the design and control of aquatic soft-bodied machines because these are often made of relatively light materials and added-mass effects become prominent when $\rho_s/\rho_f \sim 1$ or <1, with ρ_s and ρ_f being the density of the solid and the fluid.

The role that added-mass plays when a body undergoes shape variations such as those experienced by cephalopods has not been looked into in details. To do so we take in consideration the same mechanical system employed by Basset and expand

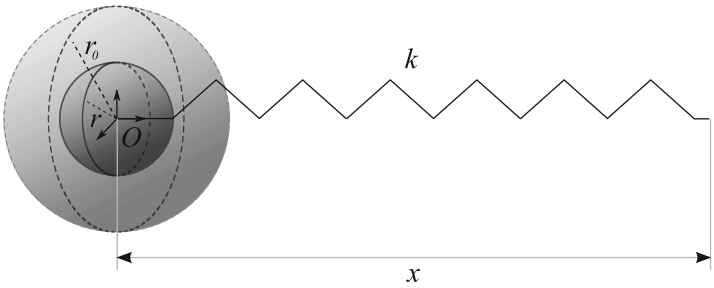

Fig. 1 Scheme of the shape-changing spring-mass oscillator. Here r represents the radius of the oscillator at time t, while r_0 refers to the mean radius of the oscillator. The distance of the frame of reference centered in O from the relaxation point of the spring is x. Adapted from [5].

on this by accounting for the capability of an oscillating body to vary its shape, and hence its added-mass, in time, see Fig. 1.

For a body immersed in a dense, viscous fluid, it has become customary to define the dynamics of such a body according to the Morison force [10], which accounts for the combined effects of added-mass and drag via their linear summation. In this case the dynamics of the 1 dof oscillator of Fig. 1 reads:

$$\frac{d}{dt}\left(m^*\dot{x}\right) = -\frac{1}{2}\rho_f C_d A\dot{x}|\dot{x}| + kx. \tag{2}$$

Where the differential sign in front of the inertial term has been retained because we are interested in accounting for bodies whose shape can be altered in time.

We perform the differentiation on the first LHS (left hand side) term while assuming the mass to remain constant (i.e. $\dot{m} = 0$) and only the shape, and hence the added-mass, to change (i.e. $\dot{m}_a \neq 0$). This situation is resemblant to the case of an oscillator being inflated/deflated by pumping a gas inside it, so that the variation of the inertia of the oscillating body is negligible. If this is the case, the buoyancy of the oscillator does vary, but since the motion of the body is purely translational along the x direction, the forces along the vertical and horizontal direction remain fully decoupled. Hence, substituting m^* into Eq. (2) and bringing the differentiation forward yields,

$$\left(m + m_a\right)\ddot{x} = -\frac{1}{2}\rho_f C_d A\dot{x}|\dot{x}| + kx - \dot{m}_a\dot{x}. \tag{3}$$

In the LHS term, $m_a(t)$, is the time-varying added-mass, while the third RHS term is the added-mass variation term which has the form of a thrust source. This latter form of Eq. (2) suggests that added-mass variation can indeed work as a propelling force as long as the motion has been initiated by some other effect, i.e. the elastic energy of a spring, in an oscillator, or the jet, in a freely swimming organism. The occurrence of the minus sign in front of the $\dot{m}_a\dot{x}$, proves that, in order for added-mass variation to act as a propelling term, $\dot{m}_a$ must be negative, thus requiring the body to shrink.

The best way to prove that the added-mass variation term can indeed provide a positive feedback on thrust is by rearranging Eq. (3) as follows:

$$(m + m_a)\,\ddot{x} = -\left(\frac{1}{2}\rho_f C_d A|\dot{x}| - \dot{m}_a\right)\dot{x} + kx. \tag{4}$$

This latest rearrangement highlights that, if added-mass variation can act as a propelling force, a function of $\dot{m}_a$ must exist according to which,

$$\dot{m}_a = \frac{1}{2}\rho_f C_d A|\dot{x}| \tag{5}$$

thus cancelling viscous drag and eventually driving the oscillator into the regime described in Eq. (1). This implies that, by virtue of external shape variation alone, a damped oscillator can be made to behave as an undamped one. This function can be readily derived by assuming the oscillator to be a sphere, whose added-mass is simply,

$$m_a = \frac{2}{3}\rho_f \pi r^3, \tag{6}$$

where $r(t)$ is the time-varying radius of the sphere. The time derivative of m_a thus reads,

$$\dot{m}_a = 2\pi\rho_f r^2 \dot{r}. \tag{7}$$

By substituting Eq. (7) into Eq. (5), the condition for zero damping is met when,

$$\dot{r} = -\frac{1}{4}C_d|\dot{x}|. \tag{8}$$

This extremely simple formulation defines the radius variation needed for a sphere oscillating in a dense medium to cancel viscous damping effects and in this way drive the system into resonance.

A closed form for the radius variation can be found by assuming a sinusoidal velocity profile of the oscillator, i.e.:

$$x = X cos\,(\omega t) \tag{9}$$

where X is the initial displacement of the oscillator. This yields the time-varying radius profile depicted in Fig. 2 for two full oscillations and four shape-variation routines. We refer to this radius-variation routine as the "step" profile. Figure 2b reports, in the lower part, the assumed oscillator velocity and, above, the non-dimensional radius profile; Fig. 2a depicts the size of the sphere at four instants throughout half an oscillation of the body. The shape of the function $r(t)$ in Fig. 2b is extremely interesting because it qualitatively resembles the activation mode of certain pulsed-jet propelled organisms. At $t/T = 0.5$ the oscillator has zero speed when the spring is fully stretched. At this stage the sphere has a radius $r = r_0 + a$

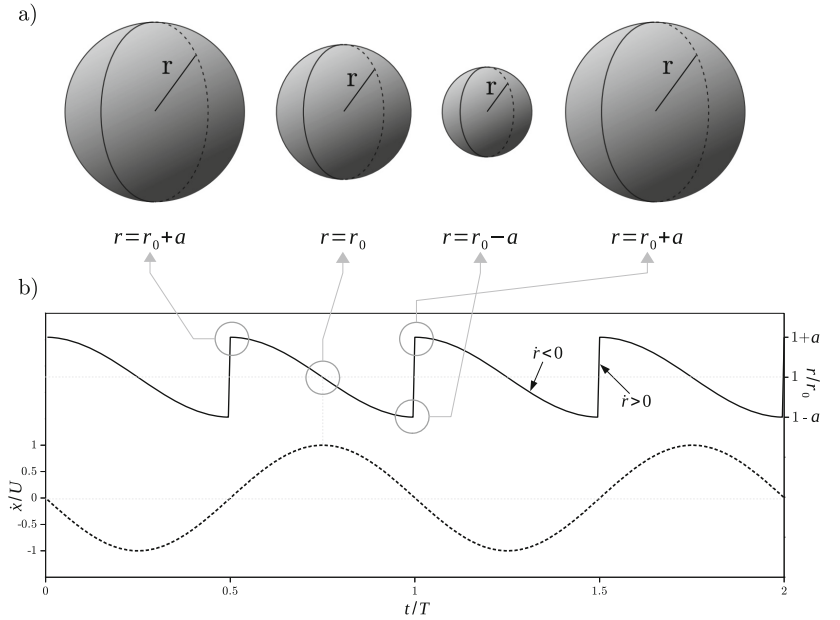

Fig. 2 Evolution in time of the shape-changing oscillator based on the "step" profile of Eq. (8). In **a**, depiction of the oscillator pulsating around the average radius r_0 at four instants during one half oscillation of the mass-spring system. In **b**, the upper part of the plot shows the profile of radius variation of the oscillator based on Eq. (8); the lower part of the plot shows the assumed velocity profile based on Eq. (9), with $U = \omega X$ being a reference velocity. Adapted from [5]

with $a = \frac{1}{4} C_d X$ being the amplitude of the radius variation of the sphere. Then the mass is released and the elastic force of the spring accelerates the sphere. Based on Eq. (8) at $t/T = 0.75$ the sphere reaches the relaxation point of the spring, where potential energy is zero, kinetic energy is maximum and the sphere has shrank to its mean value r_0. The deflation of the body continues until the end of the oscillation, $t/T = 1.0$ and $r = r_0 - a$, when the sphere stops. This is when the jump condition imposed by the absolute value in Eq. (8) forces the sphere to re-inflate abruptly to its original size. Incidentally this is the most efficient time to make the sphere inflate because if it did so during the motion, a negative thrust would be generated, slowing down the oscillation. By suddenly expanding the body when the velocity is zero, the sudden growth of added-mass has no negative impact on the propulsion. In order to verify that this kind of routine enables the oscillator to undergo resonance by annihilating viscous resistance, we perform fully coupled fluid-solid numerical simulations.

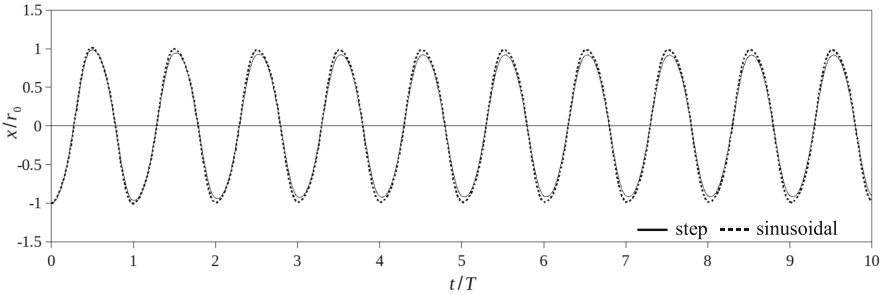

Fig. 3 Amplitude of the oscillations for the "step", Eq. (8), and "sinusoidal" shape-variation profiles obtained from the fully-coupled fluid-structure-interaction simulation. Adapted from [5].

3 Numerical Validation

To test the hypothesis formulated in Sect. 2 we use a three dimensional Navier-Stokes solver especially suited for modelling fluid-solid-interaction case studies [9, 18]. Our test case consists of a sphere in a fluid acted upon by the elastic force of a spring, Fig. 1, and a prescribed routine of pulsation based on Eq. (8) and analogous to that depicted in Fig. 2. The dynamics of the sphere is thus exclusively dependent on the spring elastic forces and the pressure forces generated by the surrounding fluid which reacts to the body displacement and body deformation.

The results, extensively discussed in [5], are briefly reported in Figs. 3 and 4a–e. The results presented in Fig. 3 confirm that the shape change of the body drives the onset of sustained resonance by acting as a propelling term or, more precisely, by cancelling the viscous damping. As opposed to the well known case of a standard weakly damped fixed-shape oscillator, where the oscillations progressively decay with time, in the pulsating case the oscillations persists while maintaining the same amplitude.

Of course, there is not one single profile of radial variation which enables recovery of kinetic energy from added-mass variation. Ideally, any pulsating mode executed at double the frequency of oscillation will drive the onset of resonance. Indeed, analogous results can be achieved by employing a "sinusoidal" radial variation profile, as demonstrated in Figs. 3 and 4f–j.

This is the first evidence of resonance being driven by the variation of added-mass, alone. These results confirm that body shape-changes can trigger an exchange of kinetic energy between the body and the fluid in such a way that it produces a positive feedback on the thrust of the body. In the case of an oscillatory system, this manifests itself in the occurrence of a resonant behaviour, but if we were dealing with a self-propelled vehicle the same phenomenon would appear as an additional source of thrust.

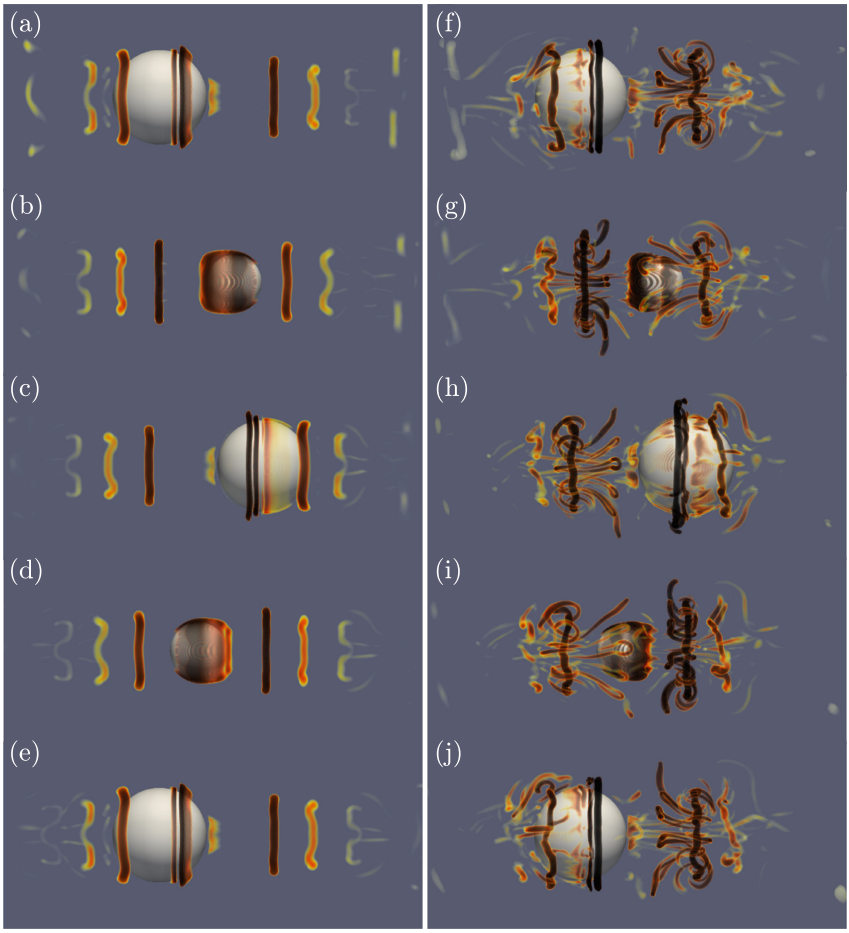

Fig. 4 Evolution of the vortical structures (λ_2 vortex criterion) during one oscillation after attainment of the zero-damping regime in response to the "step" (**a**, **b**, **c**, **d**, **e**) and the "sinusoidal" (**f**, **g**, **h**, **i**, **j**) radius variation profile at $t/T = 0.2$ (**a**, **f**), $t/T = 0.4$ (**b**, **g**), $t/T = 0.6$ (**c**, **h**), $t/T = 0.8$ (**d**, **i**), $t/T = 1.0$ (**e**, **j**). Adapted from [5].

4 Added-Mass Recovery in Self-propelled Vehicles

Evidence of the capability of a shape-changing body to benefit of thrust thanks to the recovery of kinetic energy has been demonstrated in [16]. A vehicle consisting of a rigid neutrally buoyant structure of length $L = 27\,\text{cm}$ and an elastic membrane stretched around it is used as the demonstrator. This vehicle is meant to replicate one pulsation of a cephalopod: the elastic membrane is inflated with water and, once released, the water stored inside the membrane is accelerated across a nozzle of section A_j. This jet of water pushes the vehicle forward as the elastic membrane

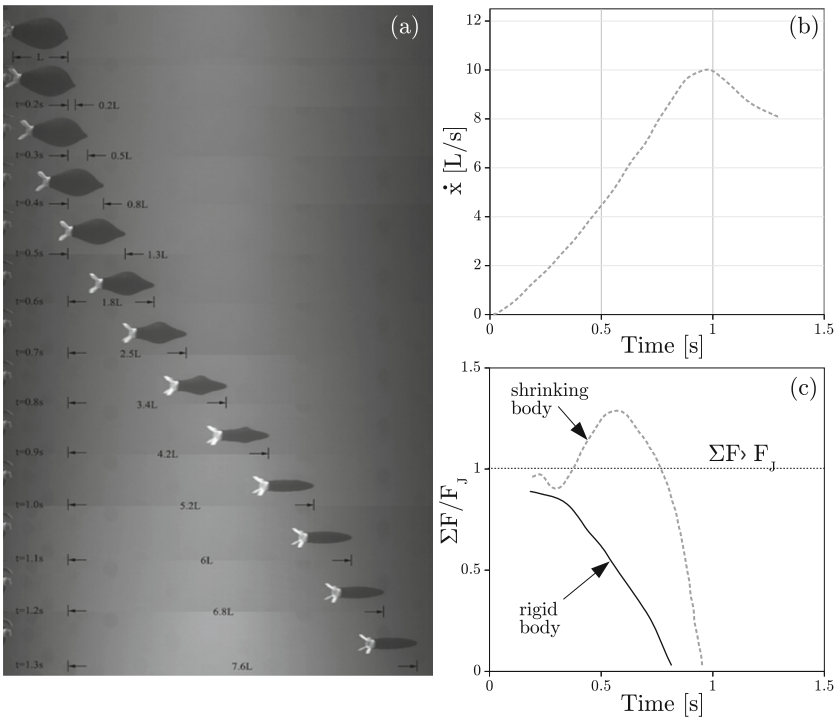

Fig. 5 Experiments performed with a shape-changing self-propelled vehicle; **a** sequential frames of the deflating vehicle, **b** speed of the vehicle as measured by tracking the center of mass of the body and **c** net thrust force non-dimensionalized by the jet force F_j for the shape-changing body (dashed gray line) compared with that experienced by a rigid 5:1 ellipsoid of revolution subject to the same jet thrust F_j. Above the $\Sigma F/F_j = 1$ line the vehicle is subject to added-mass recovery effect and the net force is larger than the jet thrust. Adapted from [16].

deflates. The experiments entail the recording of the displacement of the vehicle along with its shape deformation, Fig. 5a. Edge detection of the frames taken during this single burst of acceleration provides an accurate estimate of the membrane outline and, hence, of the instantaneous volume of the vehicle and its center of mass. From these, the ejected mass and the velocity, $\dot{x}$, of the vehicle, Fig. 5b, can be derived. The mass of the vehicle, with its payload, decreases from its starting value of $m_0 = 3.65\,\text{kg}$ to the point when the membrane comes in contact with the rigid frame; this yields an almost constant rate of mass expulsion of $\dot{m} = 3\,\text{kg s}^{-1}$. From these quantities, the thrust generated by the jet $F_j = \dot{m}U_j$, with $U_j = \frac{4}{3}\frac{\dot{m}}{\rho_f A_j}$, and the total force $\Sigma F = \dot{m}\ddot{x}$ experienced by the shrinking vehicle are derived. The force ΣF acting over the body can be compared to that experienced by a rigid 5:1 ellipsoid of revolution subject to the same F_j. The comparison is presented in Fig. 5c. The area above the line $\Sigma F/F_j = 1$ defines the dynamics regulated by the added-mass recovery effect according to which the vehicle experiences more thrust than that provided by the jet alone.

From a conservative analysis the shrinking prototype was found to benefit of a 30 % increase in thrust associated with the shape-variation alone, with a 130 % increase in acceleration with respect to the rigid case and a 200 % increase in speed. The peak shown in Fig. 5c for the shrinking body, as opposed to that of the rigid body, can only be attributed to the term $-\dot{m}_a\dot{x}$ which arose in Eq. (3) due to the shape variation of the oscillator. The dynamics observed in the shrinking vehicle can only be justified by accounting for the shape variation effects, thus confirming the role of added-mass recovery as a source of thrust.

5 Conclusion

The purpose of this study is to underline the benefit of controlled shape modification in the frame of the propulsion of deformable aquatic bodies. While it is hard to assess the role of shape change on thrust in actual self-propelled systems, the approach used here permits to segregate the effect of added-mass variation from other sources of thrust and in this way to highlight its role as a propelling force.

We provide a rigorous formulation of the phenomenon associated with shape variation by studying a simple mechanical system consisting of a spring-mass oscillator submerged in quiescent fluid and subject to periodic changes in its volume. The study of this simplified system demonstrates that the kinetic energy associated with the shape variation can completely cancel the viscous damping of the fluid, eventually giving rise to sustained, persistent oscillations. We also present experiments performed on a shape-changing self-propelled vehicle whose peculiar dynamics can only be explained by accounting for the role of added-mass recovery hereby formulated.

The confirmation that a body immersed in a dense fluid which undergoes an abrupt change of its shape experiences a positive feedback on thrust has significant implications in the design and control of soft underwater robots that exploit shape variation as their locomotion strategy.

Acknowledgments We wish to acknowledge the Natural Environment Research Council (grant number NE/P003966/1) and the Lloyds Register Foundation for their support.

References

1. Basset, A.B.: On the motion of a sphere in a viscous liquid. Philos. Trans. R. Soc. Lond. **179**, 43–63 (1888)
2. Giorelli, M., Giorgio-Serchi, F., Laschi, C.: Forward speed control of a pulsed-jet soft-bodied underwater vehicle. In: MTS-IEEE OCEANS, San Diego, CA, USA (2013)
3. Giorgio-Serchi, F., Arienti, A., Laschi, C.: Underwater soft-bodied pulsed-jet thrusters: actuator modeling and performance profiling. Int. J. Robot. Res. (2016). doi:10.1177/0278364915622569

4. Giorgio-Serchi, F., Renda, F., Calisti, M., Laschi, C.: Thrust depletion at high pulsation frequencies in underactuated, soft-bodied, pulsed-jet vehicles. In: MTS/IEEE OCEANS, Genova, Italy (2015)
5. Giorgio-Serchi, F., Weymouth, G.D.: Drag cancellation by added-mass pumping. J. Fluid Mech. **798** (2016). doi:10.1017/jfm.2016.353
6. Gosline, J.M., DeMont, M.E.: Jet-propelled swimming squids. Sci. Am. **252**, 96–103 (1985)
7. Krueger, P.S., Gharib, M.: The significance of vortex ring formation to the impulse and thrust of starting jet. Phys. Fluids **15**, 1271–1281 (2003)
8. Lighthill, M.: Note on the swimming of slender fish. Int. J. Fluid Mech. **9**, 305–317 (1960)
9. Maertens, A.P., Weymouth, G.D.: Accurate Cartesian-grid simulations of near-body flows at intermediate Reynolds numbers. J. Comput. Phys. **283**, 106–129 (2015)
10. Morison, J.R., O'Brien, M., Johnson, J., Schaaf, S.: The force exerted by surface waves on piles. Petrol. Trans. **189**, 149–154 (1950)
11. Renda, F., Giorgio-Serchi, F., Boyer, F., Laschi, C.: Locomotion and elastodynamics model of an underwater shell-like soft robot. In: IEEE International Conference on Robotics and Automation, Seattle, WA, USA (2015)
12. Renda, F., Giorgio-Serchi, F., Boyer, F., Laschi, C.: Modelling cephalopod-inspired pulsed-jet locomotion for underwater soft robots. Bioinspiration & Biomimetics **10**, 1–12 (2015). doi:10.1088/1748-3190/10/5/055005
13. Sfakiotakis, M., Lane, D.M., Davies, J.B.C.: Review of fish swimming modes for aquatic locomotion. IEEE J. Oceanic Eng. **24**(2), 237–252 (1999). doi:10.1109/48.757275
14. Triantafyllou, M., Weymouth, G., Miao, J.: Biomimetic survival hydrodynamics and flow sensing. Annu. Rev. Fluid Mech. **48**, 1–24 (2016). doi:10.1146/annurev-fluid-122414-034329
15. Trivedi, D., Rahn, C.D., Kier, W.M., Walker, I.D.: Soft robotics: biological inspiration, state of the art, and future research. Appl. Bionics Biomech. **5**, 99–117 (2008)
16. Weymouth, G., Subramaniam, V., Triantafyllou, M.: Ultra-fast escape maneuver of an octopus-inspired robot. Bioinspiration & Biomimetics **10**, 1–7 (2015). doi:10.1088/1748-3190/10/1/016016
17. Weymouth, G., Triantafyllou, M.: Ultra-fast escape of a deformable jet-propelled body. J. Fluid Mech. **721**, 367–385 (2013). doi:10.1017/jfm.2013.65
18. Weymouth, G.D., Yue, D.K.P.: Boundary data immersion method for Cartesian-grid simulations of fluid-body interaction problems. J. Comput. Phys. **230**, 6233–6247 (2011)